Sea surface emissions of HOI and I_2 explain atmospheric iodine levels

Lucy J. Carpenter[1*], Samantha M. MacDonald[2], Marvin D. Shaw[1], Ravi Kumar[2], Russell W. Saunders[2], Rajendran Parthipan[1,3] , Julie Wilson[4,1], and John. M. C. Plane[2*]

[1]*Department of Chemistry, University of York, Heslington, York YO10 5DD, UK*

[2]*School of Chemistry, University of Leeds, Leeds, LS2 9JT, UK*

[3]*Now at College of Chemical Sciences, Institute of Chemistry, Ceylon, Sri Lanka*

[4]*Department of Mathematics, University of York, Heslington, York YO10 5DD, UK*

*Correspondence to: lucy.carpenter@york.ac.uk and j.m.c.plane@leeds.ac.uk

Naturally occurring halogen gases have a substantial impact on regional, and possibly even global, tropospheric ozone levels, [1-4] thereby changing the oxidizing power of the atmosphere and reducing the global warming effects of ozone.[5] The majority of halogen-related surface ozone destruction is attributable to iodine chemistry[2], yet the budget between ocean sources of iodine and gas-phase iodine oxide radicals remains unreconciled. Historically, oceanic organoiodine emissions were believed to dominate the global iodine inventory, however recent data indicates that these are insufficient to explain reactive iodine levels in the tropical marine lower troposphere.[3,4] Here we demonstrate, using two independent measurement techniques and a kinetic model of the sea surface layer, that release of hypoiodous acid (HOI) and molecular iodine (I_2) following the reaction of ozone with iodide on the sea surface can explain the "missing" source of open ocean iodine, contributing about 75% of observed iodine oxide (IO) levels over the tropical Atlantic Ocean. We find that HOI, not previously been considered as an oceanic source of iodine, is emitted at a rate ten-fold higher than that of I_2 under ambient conditions. Our results overturn the long-held view[1,6-9] that organic iodine

compounds are the main carrier of iodine from the oceans to the atmosphere, and also reveals an important negative feedback mechanism for ozone *via* O_3-induced emission of halogens.

Laboratory studies have established that I_2 is produced following the reaction of gaseous ozone (O_3) with aqueous iodide (I^-) *via* the following basic mechanism:[10-12]

$$H^+ + I^- + O_3 \rightarrow HOI + O_2 \quad (1)$$

$$H^+ + HOI + I^- \leftrightharpoons I_2 + H_2O \quad (2)$$

Reaction (1) is believed to be the major contributor to the chemical loss of atmospheric O_3 in open ocean waters and thus to its oceanic dry deposition.[13] Whilst heterogeneous reactions of O_3 with liquid substrates are frequently observed to obey Langmuir-Hinshelwood kinetics[14] indicating a surface mechanism, there is strong evidence that reaction (1) is instead driven by fast bulk accommodation and reaction in the bulk.[15-17] In this case, the ozone deposition velocity v_d (m s^{-1}) (and hence iodine emission) is controlled predominantly by the aqueous phase resistance (Γ_s, m^{-1} s) in the surface water with a contribution from the aerodynamic resistance (Γ_a, m^{-1} s) in the overlying air layer:

$$v_d = 1/\Gamma_a + 1/\Gamma_s \quad (3)$$

$$\Gamma_s = H / \sqrt{\lambda D} \quad (4)$$

where H is the gas-over-liquid form of the dimensionless Henry's law constant, D is the molecular diffusivity of O_3 in water (m^2 s^{-1}) and λ is the integrated chemical reactivity (s^{-1}) of O_3 in seawater.

We used two independent experiments and techniques - trapping of I_2 in hexane with spectrophotometric detection (Supplementary Figure 1), and conversion of I_2 to iodine oxide particles (IOPs) followed by detection of the latter with a highly sensitive ultrafine particle sensor (Supplementary Figure 2) - to quantify emissions of gaseous iodine following ozonolysis of iodide solutions as a function of $[O_{3(g)}]$ and $[I^-]$. Both methods show that emissions of I_2 increase near linearly with both $[O_{3(g)}]$ and $[I^-]$ (Figure 1), although there is evidence of surface saturation at

higher [I^-] levels in experiments where the aqueous iodide solution was unstirred, as has been observed by other workers.[11,12]

Hypoiodous acid (HOI) is in equilibrium with I_2 (Eq. 2) with an HOI/I_2 ratio of ~ 500 in seawater (pH 8), yet has not been previously considered as a carrier of iodine from the ocean. Currently, measurements of ambient HOI concentrations are not possible due to the lack of analytical techniques with sufficient accuracy and sensitivity. Laboratory experiments using very high iodide concentrations will not capture emissions of HOI from the water surface; e.g. at mM [I^-], the equilibrium [HOI]/[I_2] ratio is < 0.01 at pH 8. Here we use two methods for HOI detection: conversion of HOI to iodophenylblue (IPB) by phenyl red (PR) followed by spectrometric detection, and selective photolysis of HOI followed by conversion to IOPs in the presence of O_3 (Supplementary Methods). Both methods confirm release of gaseous HOI following O_3 deposition to iodide solutions (Figure 1c), indicating that the high concentration of aqueous HOI at the surface compensates for its low Henry's law constant (H_{HOI} is approx. 160 times lower than H_{I2} at 293 K).

In order to understand these observations and extrapolate them to the marine environment we constructed a kinetic model of the aqueous interfacial layer. Figure 2 illustrates the main processes. The rate of gaseous iodine production depends upon the flux of O_3 into the interfacial layer, the surface [I^-] and acidity, transformations of aqueous iodine species, the gas transfer velocities of HOI and I_2, and their mixing rate from the interfacial layer to bulk water (Supplementary Methods and Table S1). The very high reactivity of O_3 with I^- and the rapid volatilization rates of evolved iodine species means that there is little competition for O_3 or iodine species with other reactants, although the former becomes important at low [I^-], as discussed below. We define the thickness of the surface aqueous layer (δ), as the reacto-diffusive length over which the O_3 + I^- reaction can occur, i.e. $\delta = \sqrt{(D/\lambda}$□.[18] Using empirical expressions for mass transfer velocities (K_t) suitable for laboratory (or environmental) conditions,[19,20] the effective volatilization rate constant is then K_t /

δ (s^{-1}). Both δ and v_d are dependent on [I^-], as are the effective volatilization rate constant of iodine species and the accumulation of O_3 in the interfacial layer.

We use the model to simulate iodine evolution as a function of [I^-] and [O_3]. Figure 1 shows that the quantity and nature of the dependence of I_2 (Figures 1a and 1b) and HOI (Figure 1c) production on [O_3] and on [I^-] from iodide solutions are captured well across a wide range of conditions, except for the unstirred experiments at high [I^-] which we attribute to saturation of the surface layer, as discussed earlier. With little or no competition for O_3 other than reaction with [I^-], I_2 production is essentially linear in $[O_3]_g$, up to any saturation limit. Both O_3 uptake and O_3 accumulation in the interfacial layer increase as a function of $\sqrt{[I^-]}$, thus the net result is a near-linear dependence of I_2 production on [I^-], with an additional influence from the dependence of iodine loss from the interfacial layer as a function of δ. The ratio of HOI to I_2 production decreases substantially at high [I^-] due to the equilibrium reaction (2). At low iodide concentrations (< approx. 1×10^{-6} M [I^-] at pH 8), the model predicts that HOI is the dominant gaseous emission.

As shown in Figure 1a, the production of I_2 from ozonolysis of iodide-spiked (1.5×10^{-5} M [I^-]) seawater solutions was a factor of 2-3 less than that from pure iodide solutions, a result very similar to the measurements of Garland and Curtis.[10] We modelled the chemical effect of seawater constituents by including (i) a loss rate of O_3 to dissolved organic material (DOM) as evident in coastal waters such that the net O_3 uptake rate doubles at 100 nM [I^-][13] (ii) a pseudo first-order loss rate for I_2 reacting with DOM[21] - the same loss rate was assumed for HOI, and (iii) equilibrium reactions of HOI and I_2 with Cl^- and Br^-.[22-24] Including these reactions resulted in a 42% increase, rather than decrease, in simulated I_2 production at seawater concentrations of [Cl^-] and DOM (compared to no Cl^- or DOM) and 1.5×10^{-5} M [I^-]. We attribute the modelled increase in I_2 production to conversion of a small fraction of aqueous HOI (the dominant aqueous iodine species after IO_3^- and I^-) to I_2 by Cl^- (reactions 19, 23 and 21 in Supplementary Table 1). An increase of I_2

emissions with [Cl^-] (0 - 0.55 M) in the absence of DOM was later confirmed by experiment. The laboratory results however show that the overall effect of seawater (compared to iodide solutions) is to suppress I_2 emissions. This indicates one or more missing processes from the model. One possibility is the physical effect of organic surfactants, which have been found to result in a decrease of gaseous I_2 emissions by a factor of two,[25] possibly through stabilization of I_2 in the liquid and/or the partitioning of I_2 to organics in the interfacial layer. Organic surfactants are known to reduce sea-air gas transfer velocities,[26] and we regard the uncertainty in the physical effect of surfactants on iodine emissions as within the widely accepted factor of two uncertainty in sea-air gas transfer velocities.[27]

We next calculate iodine production at the sea surface. Sea-air transfer rates were derived from appropriate environmental parameterizations[20] to replace the "still-air" volatilization rates. The water surface-to-bulk mixing rate was replaced by a wind speed-dependent expression for transfer velocity[28] calculated from the water-side resistance to HOI and I_2 transfer. In all other respects the model processes were the same as in the laboratory simulations. A "coastal ocean" and an "open ocean" scenario were simulated from appropriate reaction rates of iodine and O_3 with DOM (Table S1); the "coastal" I_2 and HOI fluxes were between 57 – 79 % of the open ocean emissions. This reduction in iodine production is due to the loss of interfacial ozone through reactions with DOM, although this is partly compensated for by the fact that such reactions also increase the O_3 uptake rate. We find that including I_2/HOI reduction by DOM in seawater even at upper limits[21] has a negligible effect because of the very fast transfer rates of iodine out of the interfacial layer. Across all ambient conditions the major gaseous iodine species evolved was HOI, followed by I_2. Equilibrium reactions of I_2 with Cl^- and Br^- in seawater create ICl and IBr, however the calculated gaseous emissions of these compounds were less than 1% of the total iodine flux.

The evasive fluxes of HOI and I_2 and their atmospheric implications were examined using the Tropospheric HAlogen chemistry MOdel (THAMO), a 1-D model of the marine boundary layer.[3] Figure 3a shows the calculated HOI and I_2 fluxes. These are derived according to the sea surface HOI and I_2 concentrations predicted by the interfacial kinetic model equilibrated with the atmospheric concentrations in the layer immediately above the interface calculated by THAMO. The HOI flux is suppressed in the daytime because of the build up of HOI in the atmosphere through the gas-phase chemistry of iodine and HO_x (Supplementary Figure 5). At night the HOI in the atmosphere is converted to I_2 and IBr by heterogeneous chemistry on sea-salt aerosol, so that the sea-air flux is roughly twice as large. The I_2 flux exhibits the opposite behaviour: the rapid photolysis of I_2 in the atmosphere allows a relatively large flux, compared with the night when a build up of I_2 suppresses the flux. Typical equilibrated daytime emissions are ~ 7×10^7 molecule HOI cm^{-2} s^{-1} and ~ 7×10^6 molecule I_2 cm^{-2} s^{-1}, similar to total organic iodine fluxes measured over the tropical Atlantic Ocean. [3,4,29] Algorithms expressing the sensitivity of these emissions towards levels of aqueous iodide, gaseous O_3 concentration and wind speed (the most important predicted controls) are presented in the Supplementary Information.

Once in the atmosphere, HOI and I_2 quickly photolyse, releasing I atoms that react with O_3 forming the iodine monoxide (IO) radical. Regeneration of I atoms occurs through a number of O_3-destroying catalytic cycles.[29] It was recently shown that up to 50% of day-time surface O_3 destruction in the tropical Atlantic can occur through halogen cycling, that this effect is at least regional, and predominantly (nearly 70%) is attributable to iodine chemistry.[2] A specific test of this new chemistry is whether the diurnal variation of the IO concentration that has been observed at Cape Verde[2,3] can be explained. As shown in Figure 3b, measured iodocarbon fluxes[4] sustain only about 30% of the observed IO. If the unequilibrated sea-air fluxes of HOI and I_2 are used in addition to iodocarbons, THAMO overpredicts the daytime IO concentration by about 60%.

However when equilibration with the atmosphere included, very good agreement with the observed IO is achieved. The inorganic emissions explain the majority (~ 75%) of reactive iodine.

References

1. Vogt, R., Sander, R., von Glasow R., and Crutzen, P. J., Iodine chemistry and its role in halogen activation and ozone loss in the marine boundary layer: A model study. *J. Atmos. Chem.* **32** 375-395 (1999).
2. Read, K. A. *et al.* Extensive halogen-mediated ozone destruction over the tropical Atlantic Ocean. *Nature* **453**, 1232-1235 (2008).
3. Mahajan, A. S. *et al.* Measurement and modelling of tropospheric reactive halogen species over the tropical Atlantic Ocean, *Atmos. Chem. Phys.* **10,** 4611-4624 (2010).
4. Jones, C. E. *et al.* Quantifying the contribution of marine organic gases to atmospheric iodine. *Geophys. Res. Lett.* **37**, L18804, doi:10.1029/2010GL043990 (2010).
5. Saiz-Lopez A. *et al.*, Estimating the climate significance of halogen-driven ozone loss in the tropical marine troposphere. *Atmos. Chem. Phys. Discuss*. **11**, 32003-32029 (2011).
6. Law, K. S. and Sturges, W. T. The 2006 UNEP/WMO Scientific Assessment of Ozone Depletion, Chapter 2, Halogenated Very Short-lived Substances (2007).
7. Liss, P. S. and Slater, P. G., Flux of gases across the air-sea interface. *Nature* **247**, 181–184 (1974).
8. Davis, D. *et al.* Potential impact of iodine on tropospheric levels of ozone and other critical oxidants, *J. Geophys. Res.* **101** 2135 – 2147 (1996).
9. Carpenter, L.J, Iodine in the Marine Boundary Layer, *Chem. Rev.* **103**, 4953-4962 (2003).
10. Garland, J. A., H. Curtis. Emission of iodine from the sea surface in the presence of ozone. *J. Geophys. Res*. **86**, 3183–3186 (1981).
11. Sakamoto, Y., A. Yabushita, M. Kawasaki, S. Enami. Direct emission of I_2 molecule and IO radical from the heterogeneous reactions of gaseous ozone with aqueous potassium iodide solution. *J. Phys. Chem. A.* **113**, 7707–7713 (2009).

12. Hayase, S., A. Yabushita, M. Kawasaki. Heterogeneous reaction of gaseous ozone with aqueous iodide in the presence of aqueous organic species. *J. Phys. Chem. A.* **114**, 6016–6021 (2010).
13. Ganzeveld L. *et al*. Atmosphere-ocean ozone exchange: A global modeling study of biogeochemical, atmospheric, and waterside turbulence dependencies. *Global. Biogeochem. Cycles.* **23,** GB4021 (2009).
14. Clifford, D., D. J. Donaldson. Direct experimental evidence for a heterogeneous reaction of ozone with bromide at the air-aqueous interface. *J. Phys. Chem. A.***111**, 9809–9814 (2007).
15. Garland, J. A., A. W. Elzerman, S. A. Penkett. The mechanism for dry deposition of ozone to seawater surfaces. *J. Geophys. Res.* **85**, 7488–7492 (1980).
16. Magi L. *et al*. Investigation of the uptake rate of ozone and methyl hydroperoxide by water surfaces. *J. Phys. Chem. A.* **101**, 4943–4949 (1997).
17. Rouviere, A., Y. Sosedova, M. Ammann. Uptake of ozone to deliquesced KI and mixed KI/NaCl Aerosol Particles. *J. Phys. Chem. A.* **114**, 7085–7093 (2010).
18. Davidovits P. *et al*. Mass accommodation and chemical reactions at gas-liquid interfaces. *Chem. Rev*. **106**, 1323–1354 (2006).
19. Guo, Z. N. F. Roache. Overall mass transfer coefficient for pollutant emissions from small water pools under simulated indoor environmental conditions. *Ann. Occup. Hyg.* **47**, 279–286 (2003).
20. Johnson, M. T. A numerical scheme to calculate temperature and salinity dependent air-water transfer velocities for any gas. *Ocean Sci.* **6**, 913–932 (2010).
21. Truesdale, V. W., G. W. Luther, C. E. Canosa-Mas. Molecular iodine reduction in seawater: An improved rate equation considering organic compounds. *Mar. Chem*. **48**, 143–150 (1995).
22. Margerum, D. W. *et al.* Kinetics of the iodine monochloride reaction with iodide measured by the pulsed-accelerated-flow method. *Inorg. Chem.* **25,** 4900–4904 (1986).

23. Wang, Y. L., J. C. Nagy, D. W. Margerum. Kinetics of hydrolysis of iodine monochloride measured by the pulsed-accelerated- flow method. *J. Am. Chem. Soc.* **111**, 7838–7844 (1989).
24. Faria, T., D. B. Lengyel, I. R. Epstein, K. Kustin. Combined mechanism explaining nonlinear dynamics in bromine(III) and bromine(IV) oxidations of iodide ion, *J. Phys. Chem.* **97**, 1164–1171 (1993).
25. Reeser, D. I. and D. J. Donaldson. Influence of water surface properties on the heterogeneous reaction between $O_{3(g)}$ and $I^-_{(aq)}$, *Atmos. Environ.* **45**, 6116-6120 (2011).
26. Frew, N. M. *et al.* Air-sea gas transfer: Its dependence on wind stress, small-scale roughness, and surface films. *J. Geophys. Res.* **109**, C08S17 (2004).
27. Johnson, M. T. A numerical scheme to calculate temperature and salinity dependent air-water transfer velocities for any gas, *Ocean Science* **6**, 913-932 (2010).
28. Nightingale P. D. *et al.* In situ evaluation of air-sea gas exchange parameterizations using novel conservative and volatile tracers. *Global. Biogeochem. Cycles.* **14**, 373–387 (2000).
29. Saiz-Lopez A. *et al.* Atmospheric chemistry of iodine. *Chem. Rev.*, **112**, 3, 1773–1804 (2011).

Acknowledgements

We acknowledge the UK NERC SOLAS (Surface Ocean Lower Atmosphere) programme for funding and would like to thank Dr James Lee, University of York, for loan of the O_3 generator and monitor. MDS and SMM thank the NERC for the award of PhD studentships. SMM would also like to thank Vanessa Cox for assistance with the University of Leeds experiments.

Author contributions

L.J.C and J.M.C.P. designed the experiments and S.M.M, M.D.S., R.K. and R.W.S carried them out. L.J.C. designed and implemented the interfacial model and interpreted the data. R.P. developed some of the aqueous iodine mechanism used in the interfacial model and performed aqueous iodine experiments to validate it. J.M.C.P. carried out the atmospheric modeling. J.W.

performed the linear regression modeling. L.J.C. prepared the manuscript, with contributions from all authors.

Figure Captions

Figure 1. The rate of evolution of gaseous I_2 and HOI from ozonised iodide solutions and seawater as a function of $[O_{3\ (g)}]$ and $[I^-_{(aq)}]$. (a) Emissions of I_2(g) from 1.5 x 10^{-5} M $[I^-]$ solution at pH 8 (turquoise diamonds) and in seawater spiked with 1.5 x 10^{-5} M $[I^-]$ (yellow circles) using the spectrophotometric method (both stirred experiments). The red filled squares show I_2(g) emissions from 1.0 x 10^{-7} M $[I^-]$ at pH 7 using the IOP method (unstirred experiments). (b) Gaseous I_2 production as a function of $[I^-]$ in buffered (pH 8) solutions at fixed gaseous ozone mixing ratios of 70 ppbv (spectrophotometric method, turquoise diamonds, stirred experiments) and 222 ppbv (IOP method, red filled squares, unstirred experiments). (c) Gaseous HOI production as a function of $[I^-]$ in buffered (pH 8) solutions at fixed gaseous ozone mixing ratios of 150 ppbv (spectrophotometric method: filled turquoise diamonds show stirred experiments and empty turquoise triangles show unstirred experiments) and 3.56 ppmv (IOP method, red filled squares, unstirred experiments). In each figure, error bars present the RSD of the measurements, the red dashed lines represent model simulations of the IOP experiments and the black solid lines represent model simulations of the spectrophotometric experiments as discussed in the text. The model simulations include a mixing rate of evolved iodine species from the interfacial layer to the bulk to represent experiments where the solutions were stirred, which has the effect of reducing the calculated iodine concentrations by ~40% (depending on $[I^-]$) compared to an unstirred experiment (Fig. 1c).

Figure 2. Schematic of HOI and I_2 production following the reaction of O_3 with I^- at the air-sea interface. Mass transfer from the aqueous to gas phase is denoted by K_T and mixing from the interfacial layer to bulk seawater is denoted by K_{mix}.

Figure 3. Modelled iodine chemistry at Cape Verde using the 1-D model THAMO. (a) The diurnal emission fluxes of HOI and I_2, showing the effect of equilibration with atmospheric HOI and I_2. (b) Diurnal profile of IO at a height 5 m above the ocean surface, produced by the combined emission of HOI, I_2 and organoiodine compounds (solid line); HOI, I_2 and organoiodine compounds where emission is not constrained by equilibration with atmospheric HOI and I_2 (dash-dot line); and organoiodine compounds only (dashed line). The points with error bars are measurements. [2,3]

Figures

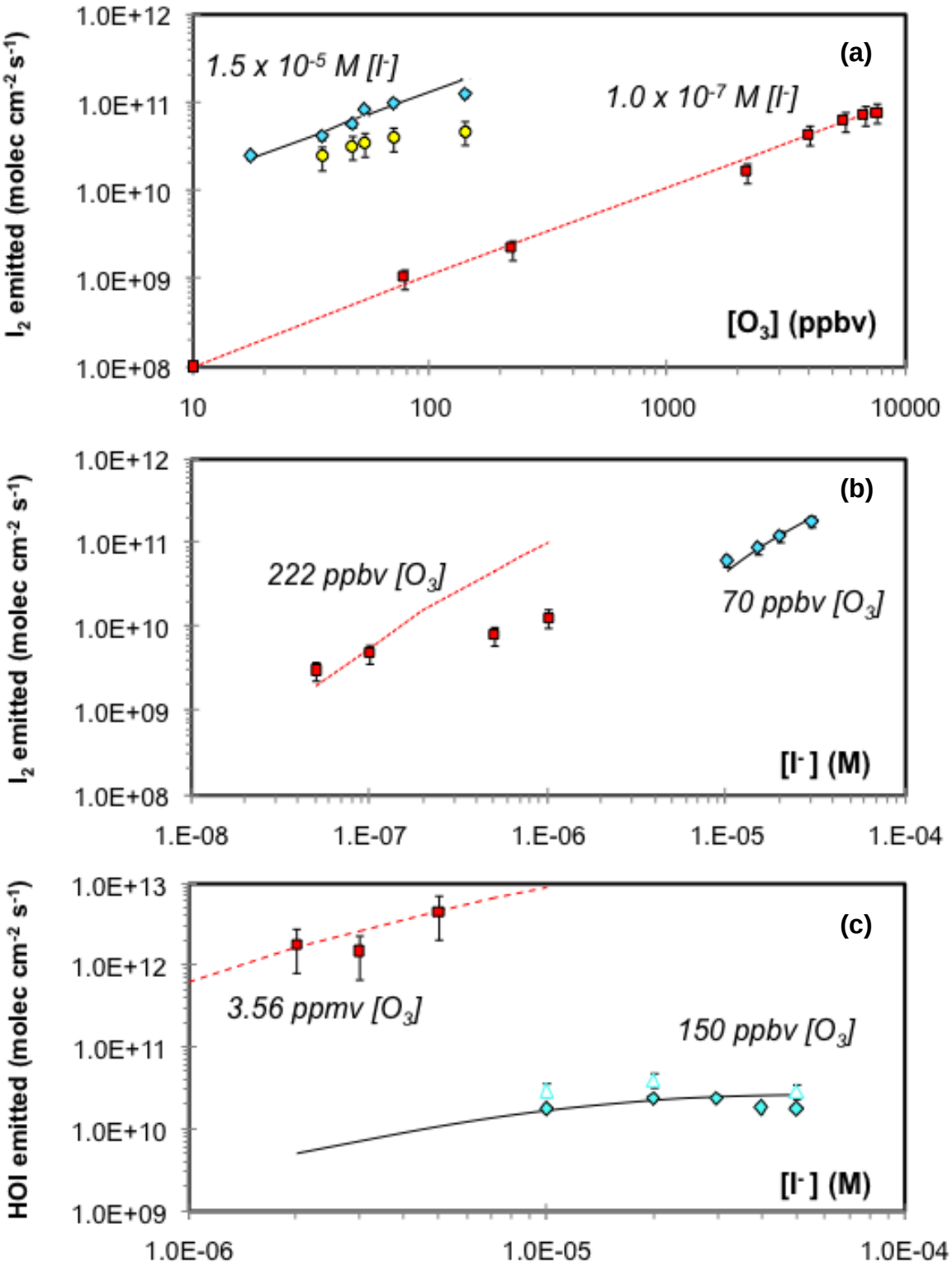

Figure 1.

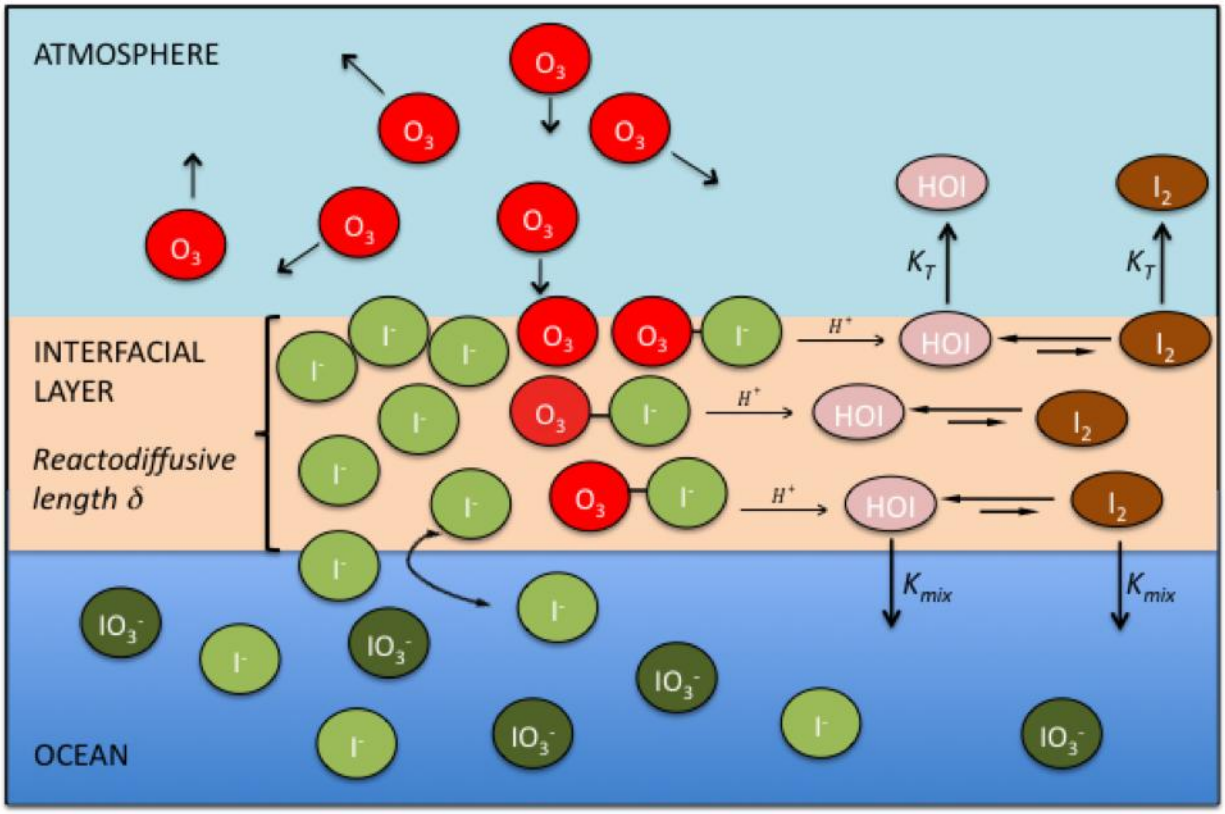
ATMOSPHERE
INTERFACIAL LAYER
Reactodiffusive length δ
OCEAN
O3
I-
IO3-
HOI
I2
H+
KT
Kmix

Figure 2.

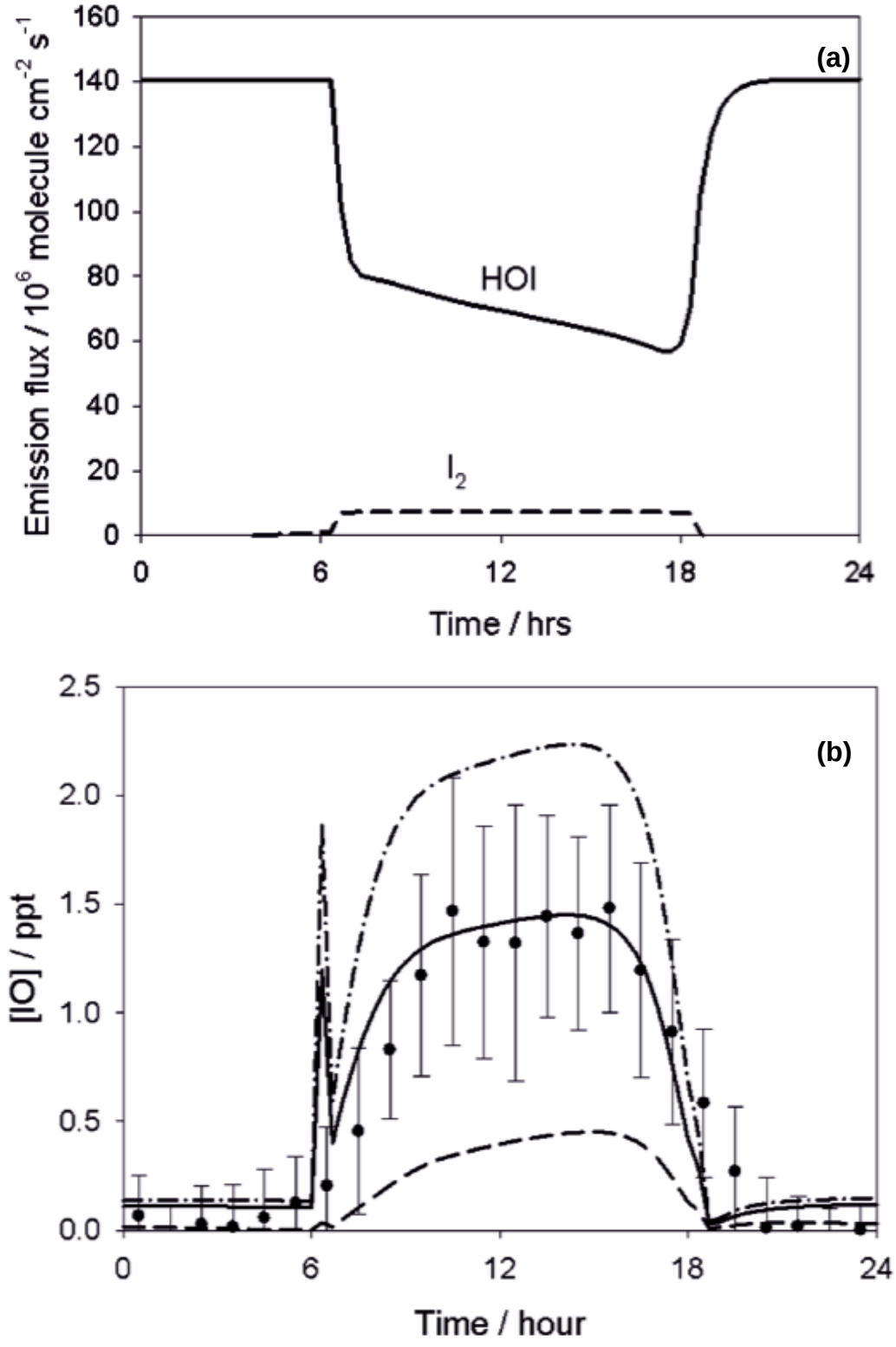
(a)
Emission flux / 10^6 molecule cm^-2 s^-1
160
140
120
100
80
60
40
20
0
HOI
I2
0
6
12
18
24
Time / hrs
(b)
[IO] / ppt
2.5
2.0
1.5
1.0
0.5
0.0
0
6
12
18
24
Time / hour

Figure 3.